10-14 July 2016, Vienna, Austria

The Fate of Trace Contaminants in a Crewed Spacecraft Cabin Environment

Jay L. Perry[1] and Matthew J. Kayatin[2]
NASA George C. Marshall Space Flight Center, Huntsville, Alabama 35812, USA

Trace chemical contaminants produced via equipment offgassing, human metabolic sources, and vehicle operations are removed from the cabin atmosphere by active contamination control equipment and incidental removal by other air quality control equipment. The fate of representative trace contaminants commonly observed in spacecraft cabin atmospheres is explored. Removal mechanisms are described and predictive mass balance techniques are reviewed. Results from the predictive techniques are compared to cabin air quality analysis results. Considerations are discussed for an integrated trace contaminant control architecture suitable for long duration crewed space exploration missions.

Nomenclature

AR	=	atmosphere revitalization
BMP	=	micropurification unit
CCAA	=	Common Cabin Air Assembly
GAC	=	granular activated carbon
ISS	=	International Space Station
LSS	=	life support system
TCC	=	trace contaminant control
TCCS	=	Trace Contaminant Control Subassembly
THC	=	temperature and humidity control
VOC	=	volatile organic compound
atm	=	atmospheres
C	=	gas phase concentration, mg/m^3
°C	=	degrees Celsius
g	=	gram
G	=	bulk gas phase molar flow rate, moles/h
h	=	hour
K	=	equilibrium constant
kg	=	kilogram
$k_H(T)$	=	Henry's Law constant at the system temperature, atm or mole/m^3-Pa
L	=	liter; bulk liquid phase molar flow rate, moles/h
M	=	molecular weight, gram/mole
m^3	=	cubic meter
mg	=	milligram
p	=	partial pressure, atm
P	=	cabin total pressure, atm
Pa	=	Pascal
r_i	=	trace contaminant generation rate, mg/h
R	=	universal gas constant, 82.06 cm^3-atm/mole-K
t	=	time, hours
T	=	temperature, Kelvin
v	=	volumetric flow rate, m^3/h
V	=	cabin volume, m^3

[1] Lead Aerospace Engineer, ECLS Systems, Space Systems Dept., NASA Marshall Space Flight Center/ES62 .
[2] Aerospace Engineer, ECLS Systems, Space Systems Dept., NASA Marshall Space Flight Center/ES62.

x = liquid phase mole fraction, dimensionless
y = gas phase mole fraction, dimensionless
α_i = fraction speciation in solution
η = decimal efficiency, dimensionless

I. Introduction

UNDERSTANDING a crewed spacecraft cabin as a unique environment must account for factors that include characterizing the trace contaminant load and the various removal routes that may exist. While passive trace contaminant control serves to minimize the load component from equipment offgassing, the human metabolic component remains.[1] The active trace contaminant control (TCC) equipment that is part of the life support system (LSS) is designed primarily to address the combined equipment offgassing and human metabolic load presented by Table 1 within acceptable cabin atmospheric quality standards. The design load model presented by Table 1 has been refined since the late 1980s to address the primary contamination control design challenges.[2-5] The active TCC equipment design must consider a variety of factors such as vehicle size, crew size, performance goals, and suitable process technologies.[6] Applying functional design margin to the active TCC equipment design accommodates load components that are difficult to quantify such as contamination released from experimental payload and vehicle system equipment as well as chemical use by the crew in the form of personal care products.

Being a part of a complex, unique environment, the active TCC equipment can receive assists in removing trace contaminants from the cabin atmosphere via incidental contaminant removal in components within the atmosphere revitalization (AR) and temperature and humidity control (THC) subsystems. While the active TCC equipment design does not take such incidental removal into account to ensure a conservative functional capability, it does provide functional margin and improves the TCC equipment's life cycle economics. Understanding the fate of trace contaminants between the basic TCC equipment and incidental removal routes can quantify the functional and operational margins for the TCC equipment. Testing on the ground as well as flight operations have yielded insight into TCC at a vehicle system level.[7, 8] The following narrative discusses aspects of system-level TCC and presents techniques to quantify incidental removal to better understand TCC equipment design functional margins.

II. Trace Contaminant Removal Mechanisms

System-level TCC consists of primary and secondary trace contaminant removal mechanisms and equipment. The primary removal mechanism is provided by the TCC equipment that is specifically designed to remove trace chemical contaminants from the cabin atmosphere. The secondary removal mechanisms are provided by AR and THC subsystem equipment and overboard atmospheric leakage. The following summarizes the primary and secondary TCC mechanisms.

Table 1. Chemical load for trace contaminant control design.

CONTAMINANT NAME		GENERATION RATE[b]	
IUPAC	**COMMON**	**OFFGASSING** (mg/day-kg)[a]	**METABOLIC** (mg/day-person)
Methanol	Methyl alcohol	1.3×10^{-3}	0.9
Ethanol	Ethyl alcohol	7.8×10^{-3}	4.3
n-butanol	Butyl alcohol	4.7×10^{-3}	0.5
Methanal	Formaldehyde	4.4×10^{-6}	0.4
Ethanal	Acetaldehyde	1.1×10^{-4}	0.6
Benzene	Benzol	2.5×10^{-5}	2.2
Methylbenzene	Toluene	2×10^{-3}	0.6
Dimethylbenzenes	Xylenes	3.7×10^{-3}	0.2
Furan	Divinylene oxide	1.8×10^{-6}	0.3
Dichloromethane	Methylene chloride	2.2×10^{-3}	0.09
2-propanone	Acetone	3.6×10^{-3}	19
Trimethylsilanol	Trimethyhydroxysilane	1.7×10^{-4}	0
Hexamethylcyclotrisiloxane	D3 siloxane	1.7×10^{-4}	0
Azane	Ammonia	8.5×10^{-5}	50
Carbon monoxide	Carbonous oxide	2×10^{-3}	18
Hydrogen	Dihydrogen	5.9×10^{-6}	42
Methane	Carbane	6.4×10^{-4}	329

a. Offgassing rate is for the mass of internal, non-structural equipment. b. Supplemented by system sources as they are identified.

A. Primary Trace Contaminant Removal Mechanisms

Primary removal mechanisms encompass the equipment specifically designed to provide the active TCC function. Aboard the International Space Station (ISS), TCC equipment is located in the U.S. Segment and Russian segment. In the U.S. Segment, the Trace Contaminant Control Subassembly (TCCS) is located in the AR subsystem racks located in Node 3 and the U.S. Laboratory. The Russian micropurification unit, known by its Russian acronym БМП (BMP), is located in the Service Module. During normal operations, one TCCS and the BMP operate in tandem.

The TCCS, shown schematically by Fig. 1, consists of fixed bed containing granular activated carbon (GAC), a thermal catalytic oxidation reactor with recuperative heat exchanger, and a post-sorbent bed containing granular lithium hydroxide (LiOH) located downstream of the catalytic oxidation reactor.[9] The total flow through the TCCS is 15.3 m^3/h. Approximately 30% of the total flow, 4.6 m^3/h, is processed by the catalytic oxidizer and post-sorbent bed. The GAC used by the TCCS is specially treated with phosphoric acid (H_3PO_4) to remove ammonia (NH_3) and also removes a broad array of volatile organic compounds (VOCs). Low molecular weight VOCs such as light alcohols and formaldehyde (CH_2O) which are poorly removed by GAC are oxidized to carbon dioxide (CO_2) and water vapor in the catalytic oxidizer. The catalytic oxidizer also oxidizes methane (CH_4), carbon monoxide (CO), and hydrogen (H_2). The TCCS has substantial capacity for NH_3 removal (~250 grams) and, therefore, provides a 100% single pass removal efficiency for the normally expected NH_3 load. Ground testing has characterized the TCCS performance for the primary design-driving compounds.[10] According to this testing, light alcohols, such as methanol, are expected to rapidly break through the GAC and reach saturation capacity within approximately one week upon installing a fresh bed. Therefore, the catalytic oxidizer provides the primary control for methanol. Ethanol reaches its saturation capacity in the GAC bed later but by late in the bed's service life the removal occurs in the catalytic oxidizer. Dichloromethane begins to reach saturation capacity after a month or two of installing a fresh GAC bed making the catalytic oxidizer the primary removal device for this compound. The catalytic oxidizer provides 100% removal efficiency for CH_4, CO, H_2, CH_2O, and other light VOCs. The oxidation efficiency for dichloromethane in the catalytic oxidizer is ~80%.

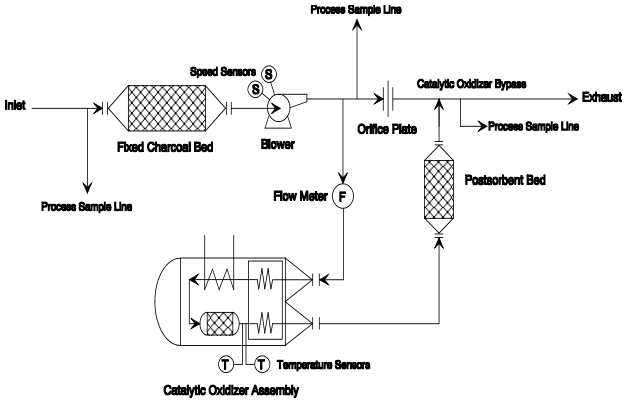

Figure 1. Simplified U.S. TCCS process diagram.

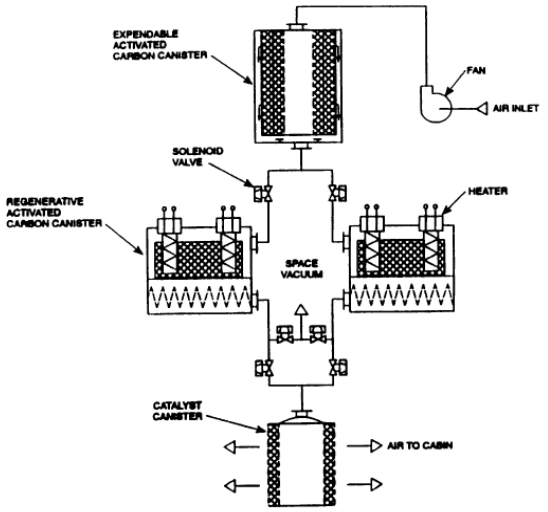

Figure 2. Simplified Russian BMP process diagram.

The BMP, shown schematically by Fig. 2., is an equipment design used aboard the Mir space station that consists of an expendable GAC canister, two regenerable GAC canisters, and an ambient temperature catalyst canister.[11] The flow through the BMP is 25 m^3/h which is higher than the unit used aboard Mir.[12] The regenerable GAC canisters are exposed to a thermal-vacuum cycle approximately every 20 days. Testing to characterize the BMP's performance was conducted in 1996.[13, 14] This testing observed high molecular weight VOC removal efficiencies consistently in the range between 90% and 100% for a normal 20-day regeneration cycle. For low molecular weight compounds such as ethanol, acetone, and ethyl acetate, the removal efficiencies fluctuate to a greater extent during the 20-day period between regeneration cycles. The average removal efficiencies for ethanol, acetone, and ethyl acetate observed during the testing were 70%, 78%, and 88%, respectively. Formaldehyde and CO removal efficiencies were observed to be >90% and 100%, respectively. Compounds such as methanol and other light VOCs are expected to reach saturation capacity for the regenerable GAC beds over the 20-day cycle; therefore, a 50% removal efficiency is typically used for these compounds. Some NH_3 removal by the expendable GAC canister up to 50% efficiency was observed during the testing.

B. Secondary Trace Contaminant Removal Mechanisms

Secondary removal mechanisms are those that remove trace contaminants from the cabin atmosphere while performing their primary function. The primary secondary removal mechanisms occur in the CO_2 removal and humidity control processes. Dilution from atmospheric gas replenishment to make up for overboard leakage also contributes. However, compared to the primary removal rate the incidental removal via dilution is very minor and is neglected in cabin mass balance calculations.

Testing has reported some net trace contaminant removal in the CO_2 removal process observed as a small VOC concentration in the CO_2 product delivered to a downstream CO_2 reduction process.[15, 16] The propagation from the process air load to the CO_2 product was approximately 5% or less. Bench scale testing with acetone and methanol showed >90% removal by the desiccant bed with subsequent desorption during the regeneration cycle.[17] This behavior stores the contaminants in the desiccant bed and then returns them to the cabin in a cyclic manner. Similar behavior was observed for these compounds as well as m-xylene during system level testing conducted in 1997.[18] More recent testing showed a similar effect with ethanol.[16] As well, observations during flight reported similar concentration dynamics for octafluoropropane.[19] Overall, observations from both ground testing and in-flight have indicated that the net incidental removal of the CO_2 removal processes is very low contributing no more than a 5% net efficiency for light VOCs. Larger VOC molecules, CH_4, CO, and hydrogen (H_2) are not removed via the CO_2 removal process.

Removal via absorption in humidity condensate is a significant secondary trace contaminant removal mechanism. In this mechanism, an equilibrium condition is approached between the contaminant concentration in the bulk process air and the condensed water. This equilibrium condition is described by Henry's Law. Removal efficiencies can range from much less than 1% to greater than 50% depending on the nature of the compound and the condensate collection process conditions. This mechanism is discussed in greater detail in Section III.

III. Incidental Removal by Humidity Control Processes

The removal of trace chemical contaminants in air via absorption by humidity condensate is a well-recognized process.[20] In this section, mass balance equations for a typical spacecraft condensing heat exchanger are presented.[21] As well, simplifying assumptions are summarized that allow the effectiveness of absorption in humidity condensate as a contamination control device to be estimated.

A. Theory and Calculation Methods

Henry's Law, defined by Eq. 1, figures prominently in developing the absorption mass balance equation.[22, 23]

$$p = k_H(T)x \tag{1}$$

In this equation, p is the partial pressure of the chemical contaminant in the bulk gas phase in atmospheres (atm), $k_H(T)$ is the Henry's Law constant at the system temperature in units of Kelvin, and x is the mole fraction of the contaminant in the bulk liquid phase. Contamination removal by a condensing heat exchanger can be described by the co-current absorption process found in Ref. 24 and illustrated by Fig. 3. Simplifying assumptions for developing the mass balance equation for a condensing heat exchanger are the following:

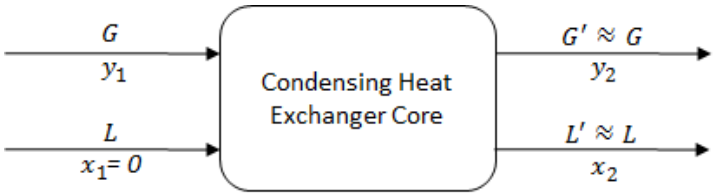

Figure 3. A simplified schematic depicting the condensing heat exchanger mass balance.

1) Bulk gas phase contaminant concentration is uniform.
2) Turbulent mixing in the heat exchanger results in a gas phase interface concentration equal to the bulk concentration making gas phase mass transfer resistance negligible.
3) Rapid mass transfer occurs at the gas-liquid interface which is governed by Henry's Law.
4) The overall process is characterized by the condensation of moisture followed by co-current absorption.
5) Low concentration of contaminants and rapid mixing in the liquid phase makes liquid phase mass transfer resistance negligible.

Equation 2 is the material balance around the condensing heat exchanger as depicted by Fig. 3. In Eq. 2, y is the gas

$$y_1G + x_1L = y_2G' + x_2L' \tag{2}$$

phase mole fraction (dimensionless), x is the liquid phase mole fraction (dimensionless), G is the inlet bulk gas phase molar flow rate (mole/h), G' is the outlet bulk gas phase molar flow rate (mole/h), L is the inlet bulk liquid phase molar

flow rate (mole/h), and L' is the outlet bulk liquid phase molar flow rate (mole/h). As depicted in Fig. 3, $x_1 = 0$, $G' \approx G$, and $L' \approx L$. Making these substitutions in Eq. 2 and solving for the outlet gas phase mole fraction, y_2, yields Eq. 3. By assuming that the liquid phase mole fraction exiting the condensing heat exchanger core, x_2, has achieved an

$$y_2 = y_1 - x_2 L/G \tag{3}$$

equilibrium condition described by Henry's Law and defining the exiting vapor phase mole fraction, y_2, as the ratio of partial pressure and total pressure, p/P, where p is the contaminant partial pressure and P is the total cabin pressure, Henry's Law becomes the following:

$$y_2 = k_H(T)x_2/P \tag{4}$$

The simultaneous solution of Eq. 3 and Eq. 4 yields Eq. 5 which is the absorption operating curve relating the exiting liquid phase mole fraction to the inlet gas phase mole fraction. Equation 5 is the basis for calculating the removal

$$x_2 = \frac{y_1}{\left[L/G + k_H(T)/P\right]} \tag{5}$$

efficiency for single pass contaminant removal via absorption in humidity condensate. The steps for calculating single pass removal efficiency based on Eq. 5 are the following:

1) Calculate the contaminant gas phase mole fraction entering the condensing heat exchanger. In Eq. 6 $C_{i,1}$ is the inlet concentration in mg/m^3, R is the universal gas constant of 82.06 cm^3-atm/mole-K, T is the cabin temperature in Kelvin, M is molecular weight in g/mole, and P is the cabin pressure of 1 atmosphere.

$$y_1 = \left(C_{i,1}RT/MP\right)\times 10^{-9} \tag{6}$$

2) Calculate the exiting liquid phase mole fraction using Eq. 5 using the gas phase mole fraction from Eq. 6.
3) Calculate the molar flow rate of the contaminant removed by the condensate collection rate based on the liquid phase mass fraction calculated from Eq. 5 where $\dot{m}_L$ is the condensate collection rate in kg/h.

$$n_i = x_2\dot{m}_L(1000/18) \tag{7}$$

4) Calculate the outlet gas phase concentration, $C_{i,2}$. In Eq. 8, v is the volumetric process gas flow rate through the heat exchanger core in m^3/h. Other terms are as they were defined in the first step.

$$C_{i,2} = \left[C_{i,1}v - \left(n_i M\right)\times 1000\right]/v \tag{8}$$

5) Calculate the decimal removal efficiency, η. The concentration terms are defined in steps 1 and 4.

$$\eta = \left(C_{i,1} - C_{i,2}\right)/C_{i,1} \tag{9}$$

This calculation sequence can be condensed into a single equation. In Eq. 10, $\dot{m}_L$ is the condensate collection rate in

$$\eta = \frac{\left(0.004558889\dot{m}_L T\right)}{\left[0.0045559\dot{m}_L TP + k_H(T)v\right]} \tag{10}$$

kg/h, T is the condensing heat exchanger operating temperature in Kelvin, P is the cabin total pressure of 1 atm, $k_H(T)$ is the Henry's Law constant in atm adjusted for the condensing heat exchanger's operating temperature, and v is the process air flow rate through the condensing heat exchanger core in m^3/h. It is important that the Henry's Law constant be adjusted for condensing heat exchanger's operating temperature and be in the proper units. The temperature adjustment is accomplished according to Eq. 11. In Eq. 11, k_H is in mol/m^3-Pa and T is in Kelvin. Reference 25 provides

$$k_H(T) = k_{H,298K}e^{\left\{\left[d\ln(k_H)/d(1/T)\right]\left(1/T - 1/298.15\right)\right\}} \tag{11}$$

an excellent compilation of values for $k_{H,298K}$ and the temperature dependence, $d\ln(k_H)/d(1/T)$. Equation 12 provides

$$k_H(T)_{atm} = \frac{1}{\left[k_H(T)_{mole/m^3\cdot Pa}\times 1.83089\right]} \tag{12}$$

the method for converting the Henry's Law constant from units of mol/m^3-Pa to atmospheres. The Henry's Law constant resulting from the temperature adjustment using Eq. 11 and unit conversion using Eq. 12 is used in Eq. 10 to calculate the single pass removal efficiency for a condensing heat exchanger.

B. Observed Humidity Condensate Loading versus Theoretical Expectations

The previously-discussed technique is used to evaluate the observed humidity condensate loading to theoretical expectations for compounds representing the most prevalent trace contaminant functional classes observed aboard the ISS—alcohols, aldehydes, ketones, aromatics, and halocarbons.[26] The compounds selected for evaluation—ethanol, acetaldehyde, acetone, m-xylene, and dichloromethane—are observed at the highest concentration in their respective functional class. In addition, ammonia, a TCC equipment design-driving compound is evaluated.

Humidity condensate composition analysis results for samples collected between March 2001 and April 2010 are considered for all compounds at a minimum. Additional humidity condensate sample analysis results through May 2015 are considered for ethanol. These results are paired with cabin atmosphere grab sample analysis results reported for samples collected within 24 to 48 hours of the humidity condensate samples.

The theoretically expected humidity condensate loading is determined based on Eq. 5 and considers the average and range of the Henry's Law constants reported in the literature. The typical condensing heat exchanger operating temperature for U.S. equipment is 4.4 °C and for the Russian equipment is 14 °C. Typical process air flow through the U.S. and Russian condensing heat exchanger cores are 339.8 m^3/h and 144 m^3/h, respectively. Average humidity condensate collection is typically 33% by U.S. condensing heat exchangers and 67% by the Russian condensing heat exchanger. Using an average 1.4 kg/person-day collection rate, a 6-crew total production of 8.4 kg/day is collected at 5.63 kg/day by the Russian condensing heat exchanger unit and 2.77 kg/day by the U.S. condensing heat exchanger units.

1. Compounds that are Stable in Water

Most humidity condensate loading calculations are straightforward because most of the VOCs of interest remain stable in water. The range of Henry's Law constants in the literature and adjusting for temperature are the primary aspects to consider.[23] Table 2 summarizes values used for assessing VOC removal by absorption in humidity condensate and predicted removal efficiencies using Eq. 10. Using Eq. 5 and the temperature and flow conditions summarized previously, the range of expected loading is obtained. Figure 4 shows the theoretical average, minimum, and maximum loading for ethanol, acetaldehyde, acetone, dichloromethane, and xylenes. The area between the minimum and maximum loading reflects the variation in Henry's Law constants reported in the literature. Overall, Fig. 4 shows that the paired humidity condensate loading and the cabin atmosphere concentrations data points typically fall within the theoretical range predicted by Henry's Law for a variety of compounds representing different chemical classes. This agreement indicates that it is appropriate to assume that the equilibrium condition described by Henry's Law is achieved in the condensing heat exchangers. Therefore, calculating single pass removal efficiency via Eq. 10 can provide an accurate result. Table 3 summarizes removal efficiencies calculated using Eq. 10 for the U.S. Common Cabin Air Assembly (CCAA) and the Russian condensing heat exchanger assembly known by the Russian acronym CKB (SKV).

Table 2. Henry's Law constants for selected VOCs, NH_3, and CO_2.

COMPOUND	HENRY'S CONSTANT, k_H*		$d\ln(k_H)/d(1/T)$	k_H at 4.4 °C	
	Average (mmole/m^3-Pa)	Range (mmole/m^3-Pa)		Average (atm)	Range (atm)
Ethanol	1712	1100 – 2300	7116.67	0.0542	0.0404 – 0.0844
Acetaldehyde	139	17 – 170	5811.11	0.925	0.756 – 1.81
Acetone	258	100 – 530	5153.33	0.587	0.286 – 1.51
Dichloromethane	3.83	2.8 – 5.7	3857.89	54.6	36.7 – 74.7
o-Xylene	2.06	1 – 3.2	4176.70	93.7	60.3 – 193
Ammonia	536	100 – 770	3971.43	0.380	0.264 – 2.03
Carbon dioxide	0.348	0.31 – 0.45	2410.00	861	666 – 967

*Constants at 298.15 K.

Table 3. Calculated condensing heat exchanger removal efficiencies for selected VOCs.

COMPOUND	CCAA EFFICIENCY (%)		SKV EFFICIENCY (%)	
	Average	Range	Average	Range
Ethanol	0.796	0.513 – 1.07	2.1	1.3 – 2.8
Acetaldehyde	0.047	0.024 – 0.058	0.114	0.058 – 0.139
Acetone	0.074	0.029 – 0.152	0.194	0.075 – 0.398
Dichloromethane	0.000796	0.000583 – 0.00118	0.00244	0.00179 – 0.00363
o-Xylene	0.000464	0.000362 – 0.00116	0.0008	0.000624 – 0.00200

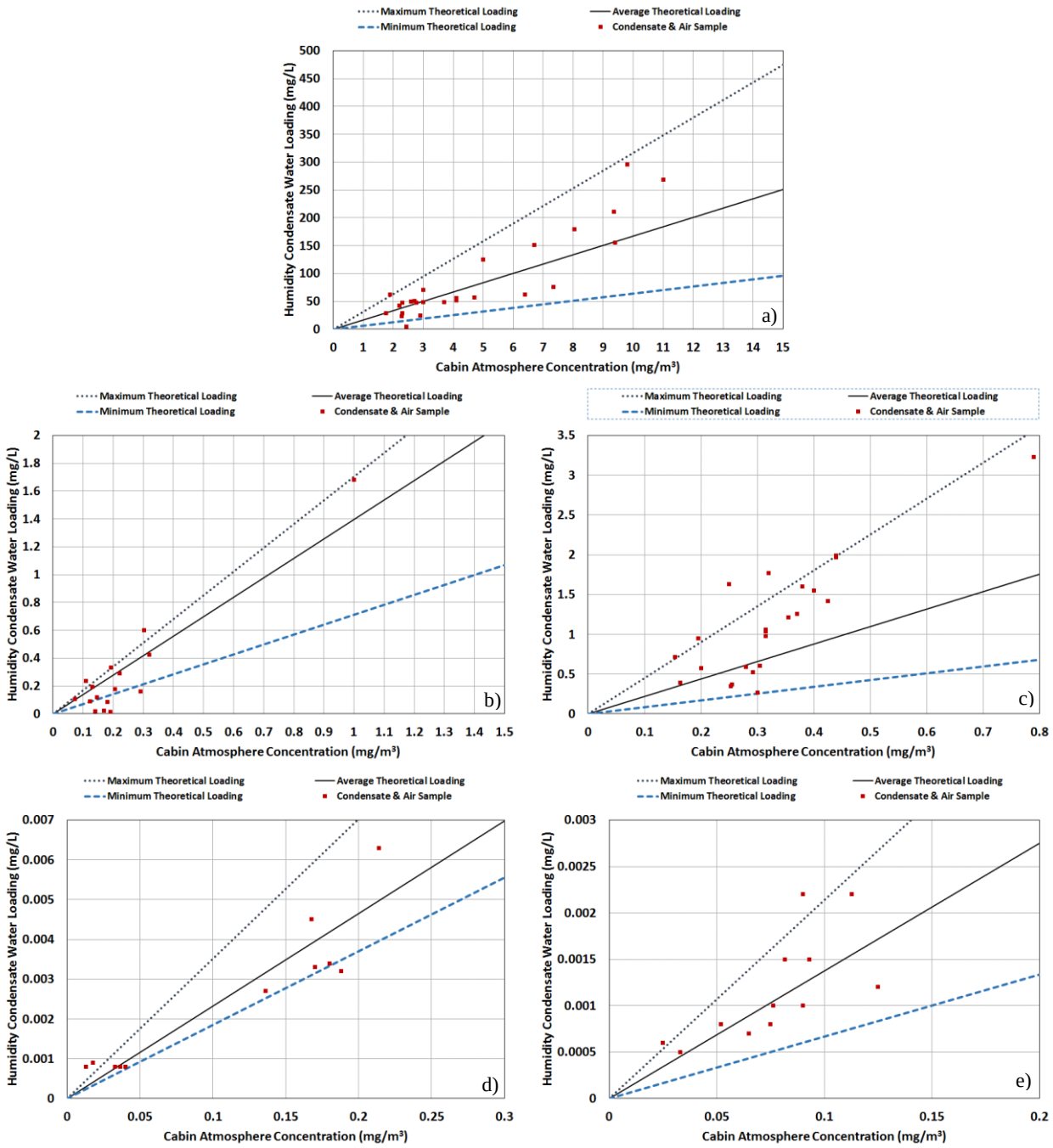

Figure. 4. Measured humidity condensate loading and cabin concentration data pairs versus Henry's Law predictions of the theoretical range around the average for compounds that are stable in water. *a) Ethanol b) Acetaldehyde c) Acetone d) Dichloromethane, and e) o-xylene. The range reflects variation in Henry's Law constants reported in the literature noted by Table 2.*

2. Compounds that Dissociate in Water

While most compounds do not interact with water, two notable compounds—NH_3 and CO_2—are weak electrolytes which partially dissociate to ionic species. In these instances, two simultaneous equilibrium conditions exist whose thermodynamics are rigorously described by Edwards et al. (1978).[27] The first is the equilibrium between the cabin concentration and the free gas in liquid solution. The second is the equilibrium between the free gas in solution and the ionized species. Henry's Law describes the first equilibrium condition between the cabin concentration and the free gas in solution. The second condition is very strongly influenced by pH and can have an effect on the free gas in

solution by affecting the mass of total inorganic dissolved species. In order to properly account for the total mass sink introduced by speciation of ions in solution, we seek to define expressions relating pH to the fractional amount of each dissolved ion at the condensate temperature. Specifically, the fraction of dissolved NH_3(aq) and CO_2(aq) are required to properly adjust Henry's Law predictions. To this end, the mathematically simpler case for monoprotic hydrolysis of the weak base NH_3 is first described which can then be logically followed by the more complex diprotic dissociation of CO_2.

In aqueous solution, absorbed NH_3 acts as a weak base leading to the formation of the ammonium ion, NH_4^+ as shown by Eq. 13.

$$NH_3(aq) + H_2O \rightleftharpoons NH_4^+ + OH^- \tag{13}$$

The temperature-dependent equilibrium or base-hydrolysis constant, K_b, can be described by Eq. 14 wherein brackets indicate the molar concentration of each species in solution.

$$K_b = \frac{[NH_4^+][OH^-]}{[NH_3]} \tag{14}$$

Definition of the formal concentration of ammonia, *i.e.* the initial, unequilibrated total moles of molecular ammonia per liter of solution, by Eq. 15 gives the required mass balance to derive the fractional speciation in solution, α_i.[28]

$$[F] = [NH_3] + [NH_4^+] \tag{15}$$

Rearrangement of Eq. 14 for $[NH_4^+]$ and substitution into Eq. 15 yields Eq. 16 upon simplification.

$$[F] = \frac{[NH_3][OH^-]+K_b[NH_3]}{[OH^-]} \tag{16}$$

Dividing Eq. 16 by $[NH_3]$ yields the definition of α_{NH3}^{-1} whose inverse is shown by Eq. 17 and defines the pH dependent speciation of unionized ammonia. Similarly, the fractional speciation of NH_4^+ can be rigorously derived but owing to its monoprotic nature is conveniently found by Eq. 18 (*i.e.* Eq. 15 normalized by [F]).

$$\alpha_{NH_3} = \frac{[OH^-]}{[OH^-]+K_b} \tag{17}$$

$$1 = \alpha_{NH_3} + \alpha_{NH_4^+} \tag{18}$$

Utilizing the relationship between pH and pOH shown by Eq. 19, the fractional dissociation curves for ammonia at

$$14 = pH + pOH \tag{19}$$

25°C are displayed by Fig. 5 wherein $K_b = 1.77 \times 10^{-5}$.[30] The intersection of the two curves in Fig. 5 defines the pKa which is approximately 9.24 at room temperature and at any pH below this value, typical for ISS condensate, NH_4^+ is the principal species in solution. For this reason, any direct measurement of $[NH_3]$ alone will significantly underestimate the total mass absorbed and at the mean ISS pH of 7.22, the error in such a measurement would be approximately 99%.

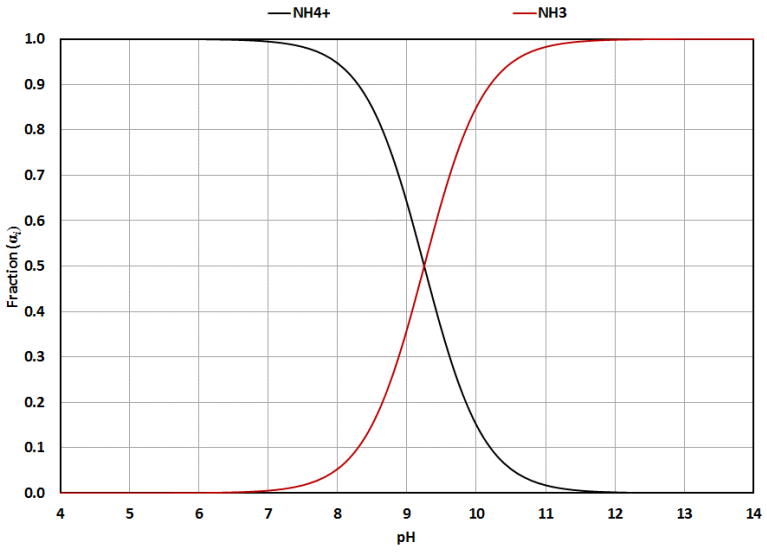

Figure. 5. The pH dependent theoretical fractional speciation of NH_3 and NH_4^+ in water at 25°C.

Absorbed CO_2 reacts with water to form carbonic acid, H_2CO_3. Carbonic acid dissociates in water to form bicarbonate HCO_3^- and, depending on pH, carbonate CO_3^{2-}. However, the concentration of H_2CO_3 is relatively small and is therefore often lumped within the term (and equilibrium constant) for aqueous carbon dioxide, $[CO_2(aq)]$.[29] Total dissolved CO_2 reacts to form HCO_3^- in accordance with Eq. 20.

$$CO_2(aq) + H_2O \rightleftharpoons H^+ + HCO_3^- \tag{20}$$

The temperature-dependent equilibrium or acid-dissociation constant, K_{a1}, can be described by Eq. 21.

$$K_{a1} = \frac{[H^+][HCO_3^-]}{[CO_2]} \tag{21}$$

Likewise, HCO_3^- can further dissociate to form CO_3^{2-} in accordance with Eq. 22 to an extent given by K_{a2} as shown by Eq. 23.

$$HCO_3^- + H_2O \rightleftharpoons H^+ + CO_3^{2-} \tag{22}$$

$$K_{a2} = \frac{[H^+][CO_3^{2-}]}{[HCO_3^-]} \tag{23}$$

Next, [F] can be defined as the stoichiometric concentration of total dissolved inorganic carbon in the system as shown by Eq. 24.

$$[F] = [CO_2(aq)] + [HCO_3^-] + [CO_3^{2-}] \tag{24}$$

Substitutions can be made in to Eq. 24 by first rearranging Eqs. 21 and 23 for $[HCO_3^-]$ and $[CO_3^{2-}]$, respectively, followed by eliminating $[HCO_3^-]$ from Eq. 23 by successive substitution to yield Eq. 25.

$$[F] = [CO_2(aq)] + \frac{K_{a1}[CO_2(aq)]}{[H^+]} + \frac{K_{a1}K_{a2}[CO_2(aq)]}{[H^+]^2} \tag{25}$$

Dividing Eq. 25 by $[CO_2(aq)]$ yields the definition of α_{CO2}^{-1} whose inverse is shown by Eq. 26 and defines the pH dependent speciation of aqueous carbon dioxide/carbonic acid.

$$\alpha_{CO_2} = 1 + \frac{[H^+]}{K_{a1}} + \frac{[H^+]^2}{K_{a1}K_{a2}} = \frac{[H^+]^2}{[H^+]^2 + K_{a1}[H^+] + K_{a1}K_{a2}} \tag{26}$$

By algebraic comparison it follows that the fractional speciation of HCO_3^- and CO_3^{2-} may be defined by Eqs. 27 and 28, respectively.

$$\alpha_{HCO_3^-} = \frac{K_{a1}[H^+\}}{[H^+]^2 + K_{a1}[H^+] + K_{a1}K_{a2}} \tag{27}$$

$$\alpha_{CO_3^{2-}} = \frac{K_{a1}K_{a2}}{[H^+]^2 + K_{a1}[H^+] + K_{a1}K_{a2}} \tag{28}$$

Figure 6 displays the fractional dissociation curves for CO_2 at 25°C with $K_{a1} = 4.45 \times 10^{-7}$ and $K_{a2} = 4.69 \times 10^{-11}$.[30] At the average observed pH of 7.22 on ISS, 88% of the dissolved inorganic carbon exists as HCO_3^-. Neglecting to include this mass at equilibrium leads to a large deviation from Henry's Law predictions. In addition, at the upper range of observed ISS pH values of 8.02, CO_3^{2-} is present at less than 1% and its influence can therefore be ignored in our analysis.

Accounting for dissociation and the effects of pH as well as temperature, an assessment of observed NH_3 and CO_2 loading in humidity condensate illustrated in Fig. 7 shows excellent agreement with theoretical predictions. The cabin concentrations for NH_3 were measured by the ANITA demonstration instrument.[31] Figure 7 accounts for the range of pH that influences the aquated free gas fraction in addition to the variation in literature Henry's Law constants.

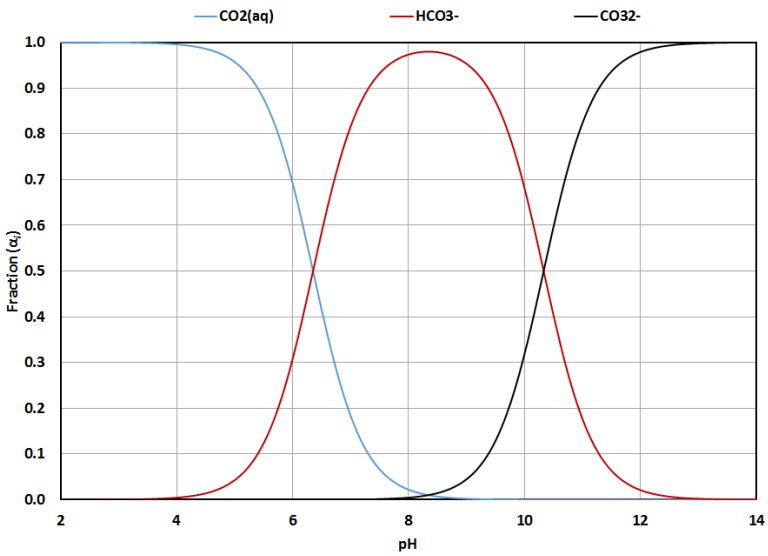

Figure. 6. The pH dependent theoretical fractional speciation of CO_2 (aq), HCO_3^-, and CO_3^{2-} in water at 25°C.

When calculating the total removal efficiency for compounds such as NH_3 and CO_2 it is necessary to recognize that the total removal is greater than what is predicted by Henry's Law alone since Henry's Law only accounts for the aquated free gas fraction in solution. The extent of dissociation must be considered for to determine the total removal and, therefore, to estimate the single pass removal efficiency. Accounting for dissociation is simple and is accomplished by dividing the efficiency calculated using Eq. 10 by the free gas fraction in equilibrium with the dissociated species as a decimal percentage. For example, the NH_3 removal efficiency for the CCAA calculated by Eq. 10 for a condensing heat exchanger removing 0.1167 kg/h of condensate with a process air flow of 339.8 m^3/h and 4.4 °C operating temperature is 0.12%. If the condensate pH is 7.22, then the free NH_3 fraction is 0.0112. The adjusted removal efficiency is obtained by dividing 0.12 by 0.0112 to yield 10.7%. The calculations yields 31.5% for the Russian SKV unit. From these calculations, the humidity control equipment represent a significant removal capacity for NH_3.

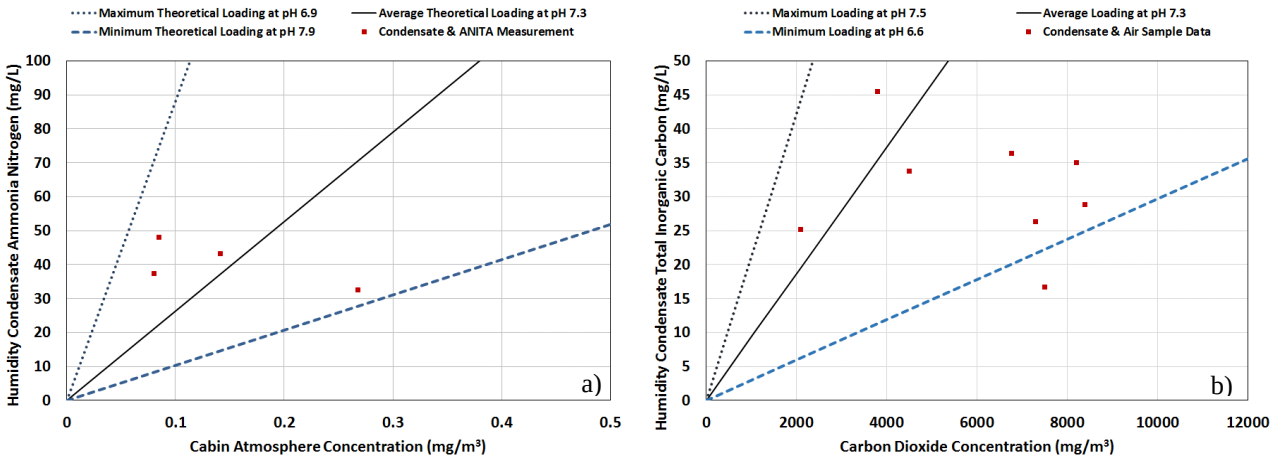

Figure 7. Measured humidity condensate loading and cabin concentration data pairs versus Henry's Law predictions of the theoretical range for compounds that dissociate in water. *a) Ammonia b) Carbon dioxide. The range reflects pH effects and the variation of Henry's Law constants reported in the literature.*

IV. Considerations for Liquid Phase Reactions

It is well understood that under certain process conditions such as concentration and pH, the interaction of species in the NH_3-CO_2-H_2O system leads to deviation from predicted Henry's Law equilibrium by formation of the carbamate ion, $NH_2CO_2^-$.[32] Equation 29 displays the reaction between NH_3 and HCO_3^-. The literature is unclear regarding the

$$NH_3 + HCO_3^- \rightleftharpoons NH_2CO_2^- + H_2O \quad (29)$$

concentration magnitude at which this reaction results in a significant deviation from Henry's Law and the single component phase equilibria described by non-interacting CO_2 and NH_3 speciation as described by Section III. For example, consider the work of Hales and Drewes (1979)[33] wherein discrepancies one order of magnitude lower than theory were observed for the solubility of NH_3 in water. This deviation was understood to result from co-absorption of atmospheric CO_2. The departure from traditional theory was believed to result from forming a volatile NH_3-CO_2 adduct although system pH was not monitored. This proposed "new" solubility theory was challenged by Ayers et al. (1985)[34] who found no deviations from Henry's Law for NH_3 loadings from 75-1200 µM in the presence of atmospheric CO_2. Later, Hales acknowledged errors in the measured solubility depression of the original work responsible for the proposed adduct formation theory.[35]

This is a significant result given the early work carried out at NASA by Kissinger et al. (1976)[36] found enhanced (3.4 times) NH_3 scrubbing potential for the Space Shuttle condensing heat exchanger as a result of NH_3-CO_2 reactions. The most dilute test condition (20 ppm NH_3) was such that extrapolation to typical cabin atmospheric concentrations <1 ppm were required. It is therefore possible that in extending empirical observations into the far dilute range of typically observed spacecraft NH_3 loadings, the regime wherein significant NH_3-CO_2 interactions exist was exited and/or extrapolation errors were introduced by the non-linear regression curves. In other words, the enhancement of NH_3 solubility does not necessarily translate to the dilute regime which in turn has tangible implications on understanding the spacecraft cabin mass balance.

In this research, two pieces of evidence suggest NH_3-CO_2-H_2O interactions are limited to binary NH_3-H_2O and CO_2-H_2O reactions alone aboard the ISS. First, while circumstantial, the reported lower experimental pH range for

ternary interacting systems is comparatively quite high at 8.59 [37] and 8.61 [32]. In both cases, the experimental load of 100 mol NH_3/L was much higher than the <3.5 mmol/L typically observed in humidity condensate aboard ISS. However, the ratios of NH_3 to CO_2 are much higher aboard ISS than in Ref. 32. A higher experimental pH is significant because NH_3 must be present in its molecular form to interact with CO_2 according to Eq. 29. The temperature-dependent equilibrium constant K_c can by defined by Eq. 30 and has a value of 3.085 at 25°C which indicates carbamate formation is favored.[38, 39]

$$K_c = \frac{[NH_2CO_2^-]}{[NH_3][HCO_3^-]} \tag{30}$$

However, at the mean observed ISS pH, the α_{NH3} is approximately 0.0087 at room temperature which at the measured condensate mass loadings limits any potential carbamate formation to the order of 10^{-8} mol/L. Therefore, even if interactions are present in the dilute regime typically observed on ISS ($[NH_3\text{-N}] \approx 100$ mmol/L; $[CO_2(aq)] \approx 1$ mmol/L) they are significantly limited by the system pH and trace condensate electrolyte loading.

V. Trace Contaminant Cabin Mass Balance

Assuming that a spacecraft cabin is a single well-mixed volume, Eq. 31 provides the mass balance for any chemical contaminant.[40] In Eq. 31, C_i is the contaminant concentration in the cabin atmosphere in mg/m^3, r_i is the contaminant

$$\frac{dC_i}{dt} = \frac{r_i}{V} - \frac{\sum \eta v}{V} C_i \tag{31}$$

generation rate in mg/h, V is the cabin free volume in m^3, and $\Sigma\eta v$ is the total active removal capacity for all known contamination control equipment removal routes in m^3/h. The solved form of this mass balance equation yields Eq. 32. In Eq. 32, C is the contaminant concentration at time, t; C_o is the contaminant concentration at time equal to zero,

$$C = C_o e^{-(\sum \eta v/V)t} + \left(r \Big/ \sum \eta v\right)\left[1 - e^{-(\sum \eta v/V)t}\right] \tag{32}$$

V is cabin volume, $\Sigma\eta v$ is the effective contaminant removal flow for all removal routes, r is the contaminant generation rate, and t is time. The rate of change for most contaminant concentrations is very slow. Therefore, Eq. 33, the steady state form of Eq. 32, can be used for most TCC calculations.

$$C = r \Big/ \sum \eta v \tag{33}$$

VI. Contaminant Generation Predicted from Cabin Mass Balance

A general cabin trace contaminant mass balance for the ISS can be accomplished using Eq. 33 and the removal efficiencies described in Section II for the TCCS and BMP and Section III for the humidity control equipment. Table 4 presents the resulting removal rates and total contaminant generation for several compounds of interest.

Comparing the total generation in Table 4 to generation rates derived from Table 1 for a total trace contaminant load consisting of offgassing from 175000 kg of equipment and the metabolic production from six crewmembers shows close agreement for NH_3 and some notable exceptions for the solvent compounds. The mass balance indicates an NH_3 load about 5% lower than the load model. Three solvent compounds—ethanol, dichloromethane, and o-xylene—have lower generation rates according to the mass balance versus the load model.

The ethanol load calculated from Table 1 is 1.39 g/day which is 1.45 g/day lower than predicted by the ISS cabin mass balance. It should be noted that the load model in Table 1 does not include cleaning solvent use aboard the ISS which is beyond the scope of the standard TCC load model. The daily ethanol usage rate for cleaning purposes is controlled within the range of 1 g/day to 2 g/day. When alcohol-based cleaning solvent use is added to the Table 1 load model, the mass balance results are consistent with the load model.

The daily generation rates for acetone, dichloromethane, and o-xylene derived from Table 1 are 75% to 82% higher than the cabin mass balance indicates in Table 4. The offgassing rate component accounts for this difference. Considering that many manufacturing and cleaning processes as well as coating, paint, and adhesive formulations have moved away from using volatile solvents over the past two decades, this difference is understandable because the design load model's context is the Shuttle and Spacelab program era when these solvents were more commonly in use.

Overall, for the compounds of interest in Table 4, the ISS cabin mass balance indicates that the design load model presented by Table 1 is reasonably conservative with the exception of needing to account for the allowed daily ethanol wipe usage cleaning purposes.

Table 4. Removal rates by different devices for average an average ISS cabin concentration.

COMPOUND	CABIN CONCENTRATION (mg/m^3)	REMOVAL RATES					TOTAL GENERATION (mg/day)
		TCCS (mg/day)	BMP (mg/day)	CCAA (mg/day)	SKV (mg/day)	OTHER (mg/day)	
Ethanol	4	440	1680	260	290	170	2840
Acetaldehyde	0.33	120	170	1.3	1.3	14	307
Acetone	0.3	110	140	1.8	2	12	266
Dichloromethane	0.12	13.2	50	0.0078	0.0101	5	68
o-Xylene	0.16	60	90	0.0061	0.0044	10	160
Ammonia	0.112	40	30	100	120	4.7	295

A further examination of Table 4 yields insight on the dominant removal routes of the trace contaminants of interest. As shown by Table 5, the active TCC equipment provides the primary removal. Combined, the TCCS and BMP are expected to remove ~93% to ~97% of the load for the aldehyde, ketone, halocarbon, and aromatic compound classes. Humidity control removes <<0.1% to ~1.5% for these compound classes. Approximately 19% of the more soluble compound load, such as ethanol, is removed by the humidity control equipment with the TCCS and BMP accounting for ~75%. Other removal routes, such as retention in CO_2 removal equipment and overboard leakage remove ~4% to ~6% of the load.

Table 5. Relative contribution of removal routes aboard the ISS.

COMPOUND	REMOVAL CONTRIBUTION				
	TCCS (%)	BMP (%)	CCAA (%)	SKV (%)	OTHER (%)
Ethanol	15.6	59.2	9.1	10.2	5.9
Acetaldehyde	38.9	55.9	0.4	0.4	4.4
Acetone	41.3	52.6	0.7	0.8	4.7
Dichloromethane	19.3	73.4	0.01	0.01	7.3
o-Xylene	37.5	58.2	0.004	0.003	4.2
Ammonia	13.8	11.2	32.7	40.8	1.6

The humidity control equipment can provide significant removal for compounds that dissociate, interact with water, or undergo liquid phase reactions such as NH_3. Table 5 shows that ~73% of the NH_3 load is removed by the humidity control equipment with the TCCS and BMP accounting for 25%.

The relative contribution to removal resulting from the mass balance compares favorably to system-level testing conducted in 1997 for the ISS Program. In this testing the TCC equipment removed ~45% to ~56% of the ketone, halocarbon, and aromatic classes, ~22% of the light alcohols, and ~23% of the NH_3. The humidity control equipment removed <<1% to 1.6% of the ketone, halocarbon, and aromatic classes, ~12% of the light alcohols, and 55% of the NH_3. The results from the cabin mass balance for relative removal percentages are similar in magnitude to these testing results as well as in the same order of precedence. Therefore, the approach to the mass balance calculation technique described herein is concluded to reasonably predict the fate of trace contaminants for a well-mixed cabin atmosphere that is maintained by both active TCC and condenser-based humidity control equipment.

VII. Summary and Conclusions

The theory and methodology for understanding the fate of trace contaminants in the unique environment of a crewed spacecraft cabin were presented and developed. The specific mass balance for co-current flow, condenser-based humidity control equipment was presented and demonstrated to accurately correlate with the observed phase equilibria humidity observed from concentrations reported in closely paired humidity condensate and cabin atmosphere samples. The considerations for addressing contaminant dissociation in the liquid phase were presented. Observations and literature indicate that the conditions typically present in a crewed spacecraft cabin do not promote interaction between NH_3 and CO_2 in the liquid phase. The approach to an overall cabin trace contaminant mass balance was presented. The mass balance technique was found to accurately predict the relative contribution to trace contaminant removal and order of precedence for primary TCC equipment and incidental trace contaminant removal by humidity control equipment for a well-mixed crewed spacecraft cabin environment.

References

[1]Perry, J.L., "Trace Contaminant Control", *Safety Design for Space Systems,* G.E. Musgrave, A.M. Larsen, and T. Sgobba, editors, Elsevier, 2009, pp. 201-207.

[2]Leban, M.I. and Wagner, P.A., "Space Station Freedom Gaseous Trace Contaminant Load Model Development," SAE 891513. *SAE 19th Intersociety Conference on Environmental Systems,* San Diego, California, 1989.

[3]Perry, J.L., Trace Chemical Contaminant Generation Rates for Spacecraft Contamination Control System Design, NASA TM-108497. National Aeronautics and Space Administration, Marshall Space Flight Center, Huntsville, Alabama, 1995.

[4]Perry, J.L., "Elements of Spacecraft Cabin Air Quality Control," NASA/TP-1998-207978, May 1998, pp. 27-33.

[5]Perry, J.L., "A Design Basis for Spacecraft Cabin Trace Contaminant Control, SAE 2009-01-2592, *SAE 39th International Conference on Environmental Systems,* Savannah, Georgia, 2009, pp. 5-7.

[6]Perry, J.L. and Kayatin, M.J., "Trace Contaminant Control Design Considerations for Enabling Exploration Missions," ICES 2015-108, *45th International Conference on Environmental Systems,* Bellevue, Washington, 2015.

[7]Tatara, J., Perry, J., and Franks, G. International Space Station System-Level Trace Contaminant Injection Test. NASA/TM-1999-209010, NASA Marshall Space Flight Center, Huntsville, Alabama; 1999.

[8]Perry, J.L., Abney, M.B., Conrad, R.E., Frederick, K.R., Greenwood, Z.W., Kayatin, M.J., Knox, J.C., Newton, R.L., Parrish, K.J., Takada, K.C., Miller, L.A., Scott, J.P., and Stanley, C.M., "Evaluation of an Atmosphere Revitalization Subsystem for Deep Space Exploration Missions," ICES 2015-107, *45th International Conference on Environmental Systems,* Bellevue, Washington, 2015, pp. 10-12.

[9]Link, D.E. and Angeli, J.W., "A Gaseous Trace Contaminant Control System for the Space Station *Freedom* Environmental Control and Life Support System," SAE 911452, *SAE 21st Intersociety Conference on Environmental Systems,* San Francisco, California, 1991.

[10]Perry, J.L., Curtis, R.E., Alexandre, K.L., Ruggiero, L.L., and Shtessel, "Performance Testing of a Trace Contaminant Control Subassembly for the International Space Station," SAE 981621, *SAE International Conference on Environmental Systems,* Danvers, Massachusetts, 1998.

[11]Mitchell, K.L., Bagdigian, R.M., Carrasquillo, R.L., Carter, D.L., Franks, G.D., Holder, D.W., Hutchens, C.F., Ogle, K.Y., Perry, J.L., and Ray, C.D., Technical Assessment of Mir-1 Life Support Hardware for the International Space Station, NASA TM-108441, George C. Marshall Space Flight Center, Huntsville, Alabama, March 1994, pp. 39-52.

[12]Joint Environmental Control and Life Support Functional Strategy Document, SSP 50623, Section 5, NASA Johnson Space Center, Houston, Texas, 2009, pp. 61-65.

[13]Test of the Russian Trace Contaminant Control System Filters, T495-51029-1, The Boeing Company, Huntsville, Alabama, 1996.

[14]Curtis, R.E., Perry, J.L., and Abramov, L.H., "Performance Testing of a Russian Mir Space Station Trace Contaminant Control Assembly," SAE 972267, *SAE 27th International Conference on Environmental Systems,* Lake Tahoe, Nevada, 1997.

[15]Perry, J., Abney, M., Frederick, K., Greenwood, Z., Kayatin, M., Newton, R., Parrish, K., Takada, K., Miller, L., Scott, J., and Stanley, C., "Functional Performance of an Enabling Atmosphere Revitalization Subsystem Architecture for Deep Space Exploration Missions," AIAA 2013-3421, *AIAA 43rd International Conference on Environmental Systems,* Vail, Colorado, 2013.

[16]Perry, J.L., Abney, M.B., Conrad, R.E., Frederick, K.R., Greenwood, Z.W., Kayatin, M.J., Knox, J.C., Newton, R.L., Parrish, K.J., Takada, K.C., Miller, L.A., Scott, J.P., and Stanley, C.M., "Evaluation of an Atmosphere Revitalization Subsystem for Deep Space Exploration Missions," ICES 2015-107, *45th International Conference on Environmental Systems,* Bellevue, Washington, 2015, p. 11.

[17]Zeppa, S.J., Molecular Sieve Contaminant Characterization Test Report, LMSC/F280519, Lockheed Missiles and Space Co., Sunnyvale, California, 1991.

[18]Tatara, J., Perry, J., and Franks, G. International Space Station System-Level Trace Contaminant Injection Test. NASA/TM-1999-209010, NASA Marshall Space Flight Center, Huntsville, Alabama; 1999.

[19]Honne, A., Kaspersen, K., and Shumann-Olsen, H., ANITA: Summary of Air Quality Measurements on the ISS, Draft 1, SINTEF, Oslo, Norway, 2008.

[20]Perry, J.L., "The Interaction of Spacecraft Cabin Atmospheric Quality and Water Processing System Performance," SAE 2002-01-2300, *SAE 32nd International Conference on Environmental Systems,* San Antonio, Texas, 2002.

[21]Perry, J.L., "Elements of Spacecraft Cabin Air Quality Control," NASA/TP-1998-207978, May 1998, pp. 145-148.

[22]Carroll, J.J., "Henry's Law Revisited," *Chemical Engineering Progress,* January 1999, pp. 49-56.

[23]Smith, F.L. and Harvey, A.H., "Avoid Common Pitfalls When Using Henry's Law," *Chemical Engineering Progress,* September 2007, pp. 33-39.

[24]Treybal, R.E. *Mass Transfer Operation,* McGraw-Hill Book Company, New York, 1980, p. 286.

[25]Sander, R., Compilation of Henry's Law Constants, Version 3.99, *Atmos. Chem. Phys. Discuss.*, 14, 29615-30521, 2014.

[26]Perry, J.L., "A Design Basis for Spacecraft Cabin Trace Contaminant Control, SAE 2009-01-2592, *SAE 39th International Conference on Environmental Systems,* Savannah, Georgia, 2009, pp. 3-5.

[27]Edwards, T. J., et al. "Vapor-liquid equilibria in multicomponent aqueous solutions of volatile weak electrolytes." *AIChE Journal* 24.6 (1978): 966-976.

[28]Harris, D.C., *Quantitative Chemical Analysis*, 6th Ed., New York, NY : W.H. Freeman and Co., 2003.

[29]Bates, Roger G., and G. D. Pinching. "Acidic dissociation constant of ammonium ion at 0 to 50°C, and the base strength of ammonia." *Journal of Research of the National Bureau of Standards* 42 (1949): 419-430.

[30]Martell, Arthur E., and Robert M. Smith. Critical stability constants. Vol. 1. New York: Plenum Press, 1974.
[31]Honne, A., Kaspersen, K., and Shumann-Olsen, H., ANITA: Summary of Air Quality Measurements on the ISS, Draft 1, SINTEF, Oslo, Norway, 2008.
[32]Holmes, Phillip E. NMR studies in the ammonia-carbon dioxide-water system. Thesis, 1995.
[33]Hales, Jeremy M., and Dennis R. Drewes. "Solubility of ammonia in water at low concentrations." Atmospheric Environment (1967) 13.8 (1979): 1133-1147.
[34]Ayers, G.P., Gillett, R.W., and Caeser, E.R., Solubility of ammonia in water in the presence of atmospheric CO_2, *Tellus*, (1985), *37B*, 35-40.
[35]Luecken, D. J., and J. M. Hales. "The effect of precipitation on the vertical profiles of atmospheric ammonia: A modeling investigation." Atmospheric Environment (1967) 20.12 (1986): 2381-2388.
[36]Kissinger, L. D., and C. E. Verostko. "Inherent Ammonia Removal Potential of the Space Shuttle Orbiter Condensing Heat Exchanger." JSC-08797. NASA, Lyndon B. Johnson Space Center: Houston, Texas (1976).
[37]Mani, Fabrizio, Maurizio Peruzzini, and Piero Stoppioni. "CO_2 absorption by aqueous NH_3 solutions: speciation of ammonium carbamate, bicarbonate and carbonate by a 13C NMR study." *Green Chem.* 8.11 (2006): 995-1000.
[38]Edwards, T. J., et al. "Vapor-liquid equilibria in multicomponent aqueous solutions of volatile weak electrolytes." *AIChE Journal* 24.6 (1978): 966-976.
[39]Beutier, Didier, and Henri Renon. "Representation of NH_3-H_2S-H_2O, NH_3-CO_2-H_2O, and NH_3-SO_2-H_2O Vapor-Liquid Equilibria." *Industrial & Engineering Chemistry Process Design and Development* 17.3 (1978): 220-230.
[40]Perry, J.L., "Elements of Spacecraft Cabin Air Quality Control," NASA/TP-1998-207978, May 1998, pp. 127-139.